Propagation of Geometric Tolerance Zones in 3D

Song-Hai Zhang[1], Qi-Hui Zhu[2], and Ralph R. Martin[3]

[1] Department of Computer Science and Technology, Tsinghua University, Beijing, 100084, China
zhangsh@cg.cs.tsinghua.edu.cn
[2] Department of Computer and Information Science, University of Pennsylvania, Philadelphia,PA 19104, US
qihuizhu@seas.upenn.edu
[3] School of Computer Science, Cardiff University, Wales, UK
ralph@cs.cf.ac.uk

Abstract. This paper considers error propagation in three dimensional geometric constructions using a geometric approach. First, we present definitions and constructions of tolerance zones for various fundamental elements in Euclidean space. Then, we study in detail the propagation of errors during several geometric computations, including the the distance between two skew lines, reflections, projections, and rotations, and we derive new tolerance zones from the old ones.

1 Introduction

Computer-aided design and other geometric application areas create a demand for efficient and robust algorithms, which must often deal with imprecisely defined data. There is a need for reliable mathematical foundations of such algorithms, and in particular an understanding of how errors propagate during a chain of calculations with imprecise data.

A commonly used approach to this problem is to use interval arithmetic, which represents imprecise floating point numbers by intervals; some of this work is specific to geometric applications [1, 3, 2, 7]. However, in general, interval methods tend to be too conservative, and overestimate the errors produced [6].

An alternative approach to dealing with errors in geometric computations is to use geometric tolerances as proposed by Wallner [9]. In this case, geometric tolerance zones are used, giving a more precise estimate of errors. They also have the important property of geometric invariance under rotations and translations, which interval methods based on coordinates do not [9]. Geometric tolerance computation and propagation have been studied in several papers, considering: errors in construction of geometric fundamental elements [6, 9], tolerances of free-form curves [6, 9], error propagation in geometric transformations [4], and geometric constraint solving [8]. However, much of this work has concentrated on two-dimensional problems.

In this paper we consider tolerance zone computation and error propagation during various geometric computations in three dimensions, including the

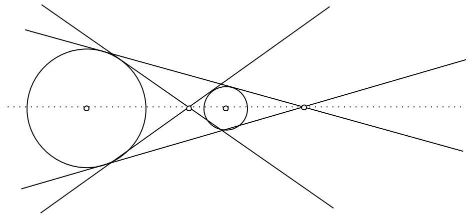

Fig. 1. Tolerance zone of line defined by two points.

distance between two skew lines, and constructions including reflections, projections, and rotations.

2 Tolerances of fundamental geometric elements

We start by defining imprecise geometric elements in three dimensions, which are the fundamental items used later in the paper. The simplest assumption to make is that the uncertainty is isotropic, i.e. an imprecisely known point lies somewhere in a sphere centred at its notional position. While this is the simplest model for a tolerance zone, other models may also be appropriate. For example, the uncertainty may be greater in a particular direction, or we may have separate ranges of uncertainty for each axis, leading to initial tolerance zones which are ellipsoidal, or box shaped, for example. In the following, we initially refer to a general 3D tolerance zone T for a point P, although later at times we assume more specifically that T is spherical, in order to provide simple results.

In many cases T may naturally be convex: for example, a sphere, ellipsoid, or polyhedron. Minkowski sums are useful when manipulating tolerance zones, as we will explain later. We note that the Minkowski sum of two convex objects is also a convex object—Minkowski sums can be computed much more easily and efficiently for convex objects than for general objects. If a tolerance zone is not naturally convex, it is often convenient to replace it by its convex hull, or some other simple convex shape, for this reason.

We start by defining the basic element, a point associated with a tolerance zone:

Definition 1. *A **fat point** is a 3D point with an associated tolerance zone T. If P is the notional position of the point, the fat point is the volume of space given by:*

$$FP(P) = \{Q | Q - P \in T\}.$$

We next define a fat line constructed from two fat points:

Definition 2. *A **fat line** is constructed from two fat points based on P_1, P_2, and is given by*

$$FL(P_1, P_2) = \{l(p_1, p_2) | p_1 \in FP(P_1), p_2 \in FP(P_2)\}$$

where $l(p_1, p_2)$ means the line through points p_1, p_2.

$FL(P_1, P_2)$ denotes the region covered by all lines having one point in $FP(P_1)$ and another point in $FP(P_2)$. Taking a specific case, if $FP(P_1)$ and $FP(P_2)$ are spherical tolerance zones, the resulting volume is bounded, in part, by two cones as shown in Fig. 1; one of the cones may degenerate into a cylinder.

We next define a fat plane constructed from three fat points:

Definition 3. *A* ***fat plane*** *is constructed from three fat points based on P_1, P_2, P_3 and is given by*

$$FPl(P_1, P_2, P_3) = \{\alpha(p_1, p_2, p_3) | p_1 \in FP(P_1), p_2 \in FP(P_2), p_3 \in FP(P_3)\}$$

where $\alpha(p_1, p_2, p_3)$ is the plane determined by three points.

When $FP(P_1)$, $FP(P_2)$, $FP(P_3)$ are all convex zones, $FPl(P_1, P_2, P_3)$ can be bounded by eight planes [6], each tangent to the tolerance zone for all three points.

Finally, we define a fat sphere with an associated tolerance zone, based on a fat point, and an uncertain radius. Let $S(P, r)$ be the sphere with centre P and radius r. Let $S^-(P, r)$ to denote its interior. Then:

Definition 4. *A* ***fat sphere*** *defined using the fat point based on P, with a radius range of $[r, R]$, is given by*

$$FS(P, r, R) = \bigcup_{p \in FP(P), l \in [r,R]} S(p, l)$$

If r is sufficiently large, and, for instance, exceeds the radius of $FP(P)$, $FS(P, r, R)$ is a hollow object. Here the radius of $FP(P)$ is defined to be half of the maximum distance between any two points on the boundary. More precisely, $FS = FS_R - FS_r$. In many cases, for simplicity of calculation, a convex polyhedron will be used as the tolerance zone for a fat point. In such a case, we may write

$$FS_R = \bigcup_{p \in FP(P)} S^-(p, R), \qquad FS_r = \bigcap_{p \in FP(P)} S^-(p, r)$$

Here, FS_R is clearly the Minkowski sum of $S^-(0, R)$ and $FP(P)$. The expression for FS_r can be simplified to

$$FS_r = \bigcap_{p \in V(P)} S^-(p, r),$$

where $V(P)$ denotes the set of vertices of $FP(P)$. FS_r could be an empty set, if r is small. We now formally state this as a theorem for the case where the tolerance zone of the fat point is a convex polyhedron, and prove it:

Theorem 1. *Given a fat sphere defined as in Definition 4, when r is larger than the diameter of $FP(P)$, $FS(P, r, R)$ can be expressed as $FS(P, r, R) = FS_R - FS_r$, where*

$$FS_r = \bigcap_{p \in V(P)} S^-(p, r).$$

.

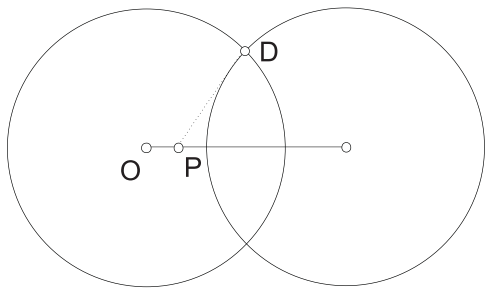

Fig. 2. Illustration of Lemma 1

Proof. It can be readily seen that

$$\bigcap_{p \in V(P)} S^-(p, r) \supseteq \bigcap_{p \in P} S^-(p, r) = FS_r.$$

Thus, we have to prove the fact that $\forall p \in P$,

$$\bigcap_{q \in V(P)} S^-(q, r) \subseteq S^-(p, r)$$

and hence the validity of

$$\bigcap_{p \in V(P)} S^-(p, r) \subseteq \bigcap_{p \in P} S^-(p, r) = FS_r.$$

We do so using the following three lemmas:

Lemma 1. *In two dimensions, let $C^-(P, r)$ denote the interior of the circle centred at P with radius r. Any point P on the line segment between any two points P_1 and P_2 must satisfy $C^-(P, r) \supseteq C^-(P_1, r) \cap C^-(P_2, r)$.*

Proof. If $C^-(P_1, r) \cap C^-(P_2, r) = \emptyset$, then the lemma is obviously correct. Otherwise, we construct a circle centre O with radius r at either end of the line segment (O is P_1 or P_2). See Fig. 2. P is an arbitrary point on the line segment. Assume P is in the interior of the circle with center P_1, we can easily see that the intersection of the two circles centered at P_1 and P_2 respectively lies within the circle centered at P: distance PD is smaller than distance OD, i.e. $PD < r$. By symmetry, the same holds if P is in the interior of the circle with centre P_2. $\square$

Lemma 2. *Generalising Lemma 1 to three dimensions for a sphere, $S^-(P, r) \supseteq S^-(P_1, r) \cap S^-(P_2, r)$.*

Lemma 3. *Let $V(M)$ be the vertex set of a polygon M. Given a point P inside the polygon M, Then*

$$S^-(P, r) \supseteq \bigcap_{Q \in V(M)} S^-(Q, r).$$

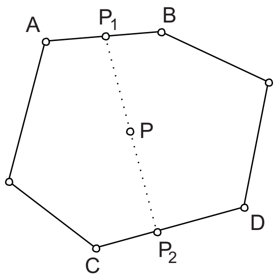

Fig. 3. Illustration of Lemma 3

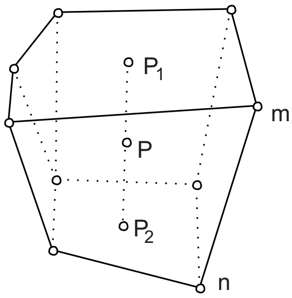

Fig. 4. Convex polyhedron

Proof. Construct some line through P that meets the boundary of the polygon at points P_1, P_2, on edges AB and CD, as shown in Fig. 3. According to Lemma 2,

$$S^-(P,r) \supseteq S^-(P_1,r) \cap S^-(P_2,r)$$

and

$$S^-(P_1,r) \supseteq S^-(A,r) \cap S^-(B,r), \quad S^-(P_2,r) \supseteq S^-(B,r) \cap S^-(C,r),$$

so

$$S^-(P,r) \supseteq S^-(A,r) \cap S^-(B,r) \cap S^-(C,r) \cap S^-(D,r) \supseteq \bigcap_{Q \in V(M)} S^-(Q,r).$$

□

We now complete the proof of Theorem 1. For a point inside the polyhedron representing the tolerance zone of the fat point, construct some line intersecting the faces of the polyhedron at P_1, P_2, as shown in Fig. 4. Using Lemmas 2 and 3, the following statements may now be proved in turn:

$$S^-(P,r) \supseteq S^-(P_1,r) \cap S^-(P_2,r),$$

$$S^-(P_1,r) \cap S^-(P_2,r) \supseteq \bigcap_{p \in V(m)} S^-(p,r) \cap \bigcap_{p \in V(n)} S^-(p,r),$$

$$\bigcap_{p\in V(m)} S^-(p,r) \cap \bigcap_{p\in V(n)} S^-(p,r) \supseteq \bigcap_{p\in V(M)} S^-(p,r),$$

as required. □

We now give an alternative definition of a fat sphere based on four fat points.

Definition 5. *The* ***fat sphere*** *generated by four fat points based on P_1, P_2, P_3, P_4 is given by*

$$FS(P_1,P_2,P_3,P_4) =$$
$$\{\sigma(p_1,p_2,p_3,p_4)|p_1 \in FP(P_1), p_2 \in FP(P_2), p_3 \in FP(P_3), p_4 \in FP(P_4)\}$$

where $\sigma(p,q,r,s)$ is the function which constructs a sphere through four points p, q, r, s.

We may now state the following theorem, assuming that the fat points in this case have spherical tolerance zones:

Theorem 2. *$\partial FS(P_1,P_2,P_3,P_4) \subseteq \Sigma$ where Σ is a set comprising 16 spheres that are each tangent to $FP(P_i)$, $i = 1,\dots,4$.*

Proof. Suppose P is an arbitrary point on the boundary of the fat sphere. Let Ω be a sphere passing through P, determined by 4 points A, B, C, D, one from each fat point zone respectively. We will prove that Ω is tangent to all 4 fat zones. Let $\Omega(A)$ be a sphere passing through A and intersecting the other three fat point zones. Perform a polar transformation with center at A, so all spheres passing through A transfrom into planes and spheres not passing through A remain spheres afterwards. After this transformation, $\mathcal{P}(FP(P_i))$ are still spheres. $\mathcal{P}(\Omega(A))$ is a plane passing through A. In particular, $\mathcal{P}(\Omega(A))$ is the fat plane passing through the three spheres which are the images of three fat points under polar transformation. After polar transformation, if a point is originally interior to a sphere, it remains interiority to the image of the sphere. Points P in $(\Omega(A))$ are boundary points of the fat sphere if under polar transformation, there exists a plane passing through P', the image of P, which is tangent to images of three spheres. Thus, $\Omega(A)$ is tangent to all the spheres. More precisely, the boundary of the fat sphere is composed of 16 common tangent spheres: each sphere has two types of tangency, so four spheres have 16 different tangent spheres. □

3 Tolerance Zones and Geometric Computations in 3D

We now consider various geometric computations in three dimensions when performed on objects defined with respect to tolerance zones.

3.1 Skew line detection and distance computation

This section considers the issue of deciding whether two fat lines intersect, and the distance between two skew lines, assuming they are based on points with

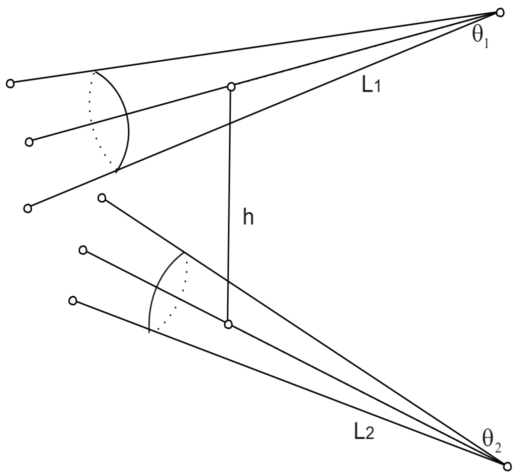

Fig. 5. Distance between two cones

spherical tolerance zones. We combine the detection and distance computation into one algorithm. We assume the two fat lines are skew lines; if their distance is negative, then the lines intersect.

A continuity argument shows that the distance between two skew fat lines may be represented by a *single* interval, i.e. it can take on any value between a minimum, and a maximum, value.

As explained earlier, a fat line determined by two fat points is bounded by two cones. We compute the distance interval by considering pairs of defining cones, one from each fat line.

Thus, all we must consider is the maximum and minimum distance between two cones. Let θ_1, θ_2 denote the semi-angles of the two cones. and let h be the skew distance between their axes (see Figure 5). O_1 and O_2 are two origins, and l_1 and l_2 are two axes. Suppose points P_1 and P_2 lie on the two cones respectively, and the distance between these two points is minimum (or maximum). These points must satisfy:

1. P_1 and P_2 lie on the cone surfaces;
2. the line P_1P_2 is normal to the cones at P_1 and P_2, so it also passes through axis of each cone. Thus, the angle between line P_1P_2 and l_1 is $\pi/2 \pm \theta_1$, and the angle between line P_1P_2 and l_2 is $\pi/2 \pm \theta_2$.

Only lines *on* the cones need be considered to calculate maximum and minimum distances. Each fat line has two cones, so there are 4 combinations of cones to consider. We call the interval formed from the maximum and minimum distance arising from one combination a *partial distance* $[d_i^{\min}, d_i^{\max}]$. The continuity argument given before shows that the final result $[D_{\min}, D_{\max}]$ must be the union of these four intervals. The main problem is now to compute $d_i^{\min}$ and $d_i^{\max}$ for each pair of cones. This calculation can be done as a special case of the

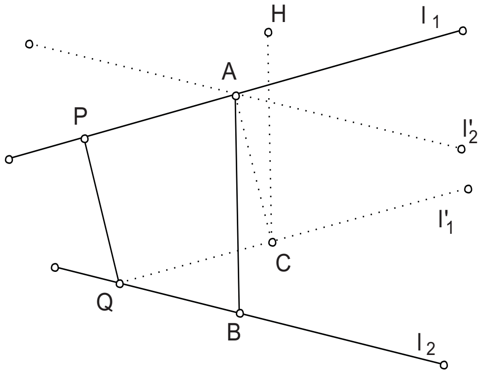

Fig. 6. Distance between two skew lines

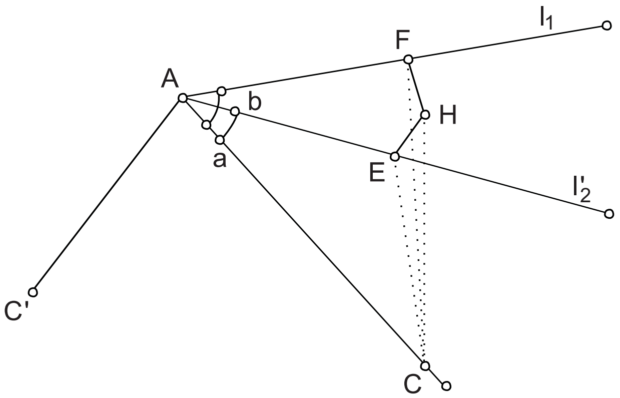

Fig. 7. Two possibilities for AC

method given in [5], which considers the distance between a canal surface and a simple surface. Here we give an alternative, direct, approach.

See Figure 6. The axes of the cones under consideration are l_1, l_2, and their semi-angles are θ_1, θ_2. Points A and B are are the points of closest approach of the two axes (the distance between them is h). Points P and Q are the points where the line P_1P_2 meets each axis l_1, l_2 respectively. Note that the angles between PQ and l_1, l_2 respectively are $\frac{\pi}{2} - \theta_1$, $\frac{\pi}{2} - \theta_2$. Construct l'_1, l'_2 parallel to l_1, l_2, so that l'_2 meets l_1 in A and l'_1 meets l_2 in Q. Shift PQ to AC. AC is now either a minimum or maximum distance between two cones (equal to PQ). as desired. The distance CH, from C to the plane determined by l_1 and l'_2, is exactly h, the extremal distance between the axes.

Figure 7 shows in further detail how to compute AC, and the extremal distance. The angles between AC and l_1, l_2 are $\pi/2 \pm \theta_1$, $\pi/2 \pm \theta_2$ respectively, giving four possible cases to consider for AC. Construct the projections E and F of H on l_1 and l'_2 on the given plane. CF and FH, and CE and EH are both

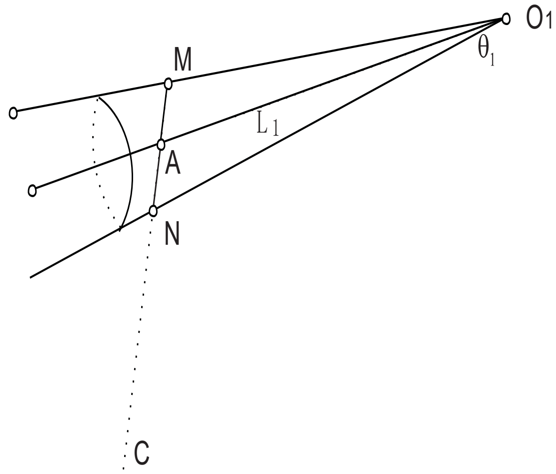

Fig. 8. the Distance inside cones

perpendicular to l_1, and l_2 respectively. The following formulae can be obtained, starting from $AC = D$, $CH = h$, and θ is the angle between l_1 and l_2':

$$AE = D\cos a, \quad AF = D\cos b, \quad EF = D\sqrt{\cos^2 a + \cos^2 b - 2\cos a\cos b\cos\theta},$$

$$AH = \frac{D\sqrt{\cos^2 a + \cos^2 b - 2\cos a\cos b\cos\theta}}{\sin\theta},$$

$$h = CH = \sqrt{D^2 - AH^2} = \frac{D\sqrt{\sin^2\theta - \cos^2 a - \cos^2 b + 2\cos a\cos b\cos\theta}}{\sin\theta},$$

$$D = \frac{h\sin\theta}{\sqrt{\sin^2\theta - \cos^2 a - \cos^2 b + 2\cos a\cos b\cos\theta}},$$

Substituting $a = \pi/2 \pm \theta_1$, $b = \pi/2 \pm \theta_2$, in which θ_1, θ_2 are acute angles, we get

$$D = \frac{h\sin\theta}{\sqrt{\sin^2\theta - \sin^2\theta_1 - \sin^2\theta_2 \pm 2\sin\theta_1\sin\theta_2\cos\theta}}.$$

In addition, the lengths of the line segments inside each cone must be added or subtracted from D to give the overall maximal or minimal distance (see Figure 8). These segments are AM and AN and their lengths should be added to or subtracted from AC: note that AC is perpendicular to O_1M. We can easily find that

$$AM = O_1A/\sin\theta_1$$

$$AN = O_1A(\tan 2\theta_1/\cos\theta_1 - \sin\theta_1).$$

Determination of whether addition or subtraction is required depends on the relative positions of AC and the cone axis l_1.

The distance between two fat lines $[D_{\min}, D_{\max}]$ can thus be computed by combining four groups of minimum and maximum distances between cones.

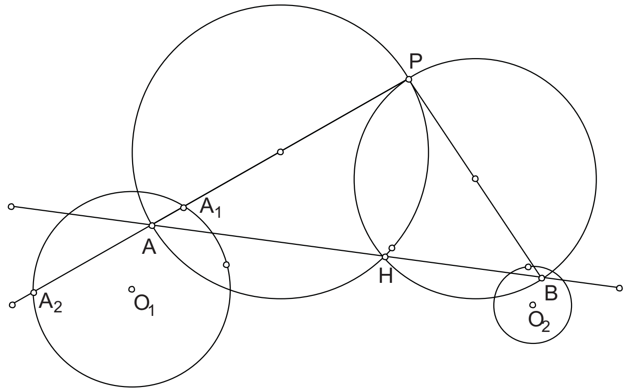

Fig. 9. Illustration of Theorem 3

3.2 Reflection and line projection in 2D

In this section we consider how to reflect an exact point in a fat line in 2D, using circular tolerance zones. A closely related problem is that of projecting an exact point onto a fat line in 2D: the projection of a point onto a line is the midpoint of the line joining the point and its reflection. Thus, a solution to either problem gives a solution to the other. Here, we consider 2D projection of an exact point onto a fat line; we then extend the ideas into 3D space in the next section.

If we wish to project a *fat* point onto a fat line, this can readily be done if the fat point is represented by a convex polygon. The tolerance zone of the projection can be found by computing the hull of the tolerance zones of the projection of each vertex of the polygon. The case in which the fat point is defined as a circular tolerance zone is more complicated, however, and further work is needed.

We start by giving a theorem concerning projection of an exact point P in a fat line.

Theorem 3. *Suppose we are given a 2D fat line $FL(O_1, O_2)$ defined in terms of two fat points with circular tolerance zones $FP(O_i)$, with O_i as center, and r_i as radius respectively. The boundary of the projection of an exact point P in this fat line can be expressed as a pair of curves $\rho = -l\cos\theta \pm r_i$, $i = 1, 2$ in polar coordinates, where the origin of polar coordinates is placed at P, and O_1P, O_2P are taken as $\theta = 0$ axes respectively.*

Proof. It can be easily seen that under projection, P goes to a region which is the intersection of two heart-shaped zones (H-zones for short), H_1, H_2 where H_i is the set of points H such that H is on the circumference of a circle with diameter PA, and $A \in FP(O_i)\}$. As Figure 9 shows, H is the projection point corresponding to some definite line joining some point A in $FP(O_1)$ to some point B in $FP(O_2)$: $PH \perp AH$ and $PH \perp BH$. Thus H belongs to both H_1 and H_2. We now consider how to calculate these two H-zones H_1, H_2.

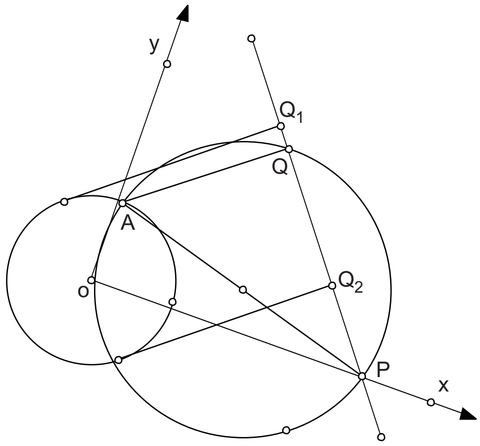

Fig. 10. Computation of inner and outer boundaries of H-zones

See Figure 10, where O corresponds to either O_1 or O_2, i.e. the tolerance zone for either of the fat points. Construct a circle of diameter of PA, where A is an arbitrary point inside circle O. This circle intersects a line l passing through P at Q with $AQ \perp l$, i.e. Q is the projection of A on l. The H-zone consists of the envelope of all such circumferences. No point inside circle O can have a corresponding point Q which lies outside the line segment Q_1Q_2, bounded by the tangents to $FP(O)$ as shown in Figure 10. As l rotates through an angle ranging from $-\pi/2$ to $\pi/2$, the positions of Q_1 and Q_2 sweep out the inner and outer boundaries of the H-zone.

If l has an angle given by θ in polar coordinates with line PO, $\theta \in [-\pi, \pi]$. In polar coordinates r is the radius of circle O. Thus, we have

$$\overrightarrow{PQ_1} = -\overrightarrow{PO}\cos\theta + r,$$
$$\overrightarrow{PQ_2} = -\overrightarrow{PO}\cos\theta - r.$$

Hence the boundaries of the H-zone are $\rho = -\overrightarrow{PO_i}\cos\theta \pm r_i$, $i = 1, 2$. □

Having found the projection of a point in a fat line, it is now straightforward to find the corresponding regions for *reflection* of a point in a fat line. The equations are simply:

$$\rho = -2\overrightarrow{PO_i}\cos\theta \pm 2r_i, \quad i = 1, 2.$$

3.3 Reflection and plane projection in 3D

We now consider projection and reflection of a point in a fat plane in 3D. Theorem 3 can be generalized as follows:

Theorem 4. *The tolerance zone formed by projection of a point P onto a fat plane in 3D is surrounded by 6 surfaces with equations in polar coordinates:*

$$\rho = l\cos\theta\cos\varphi \pm r_i, \quad i = 1, \ldots, 3$$

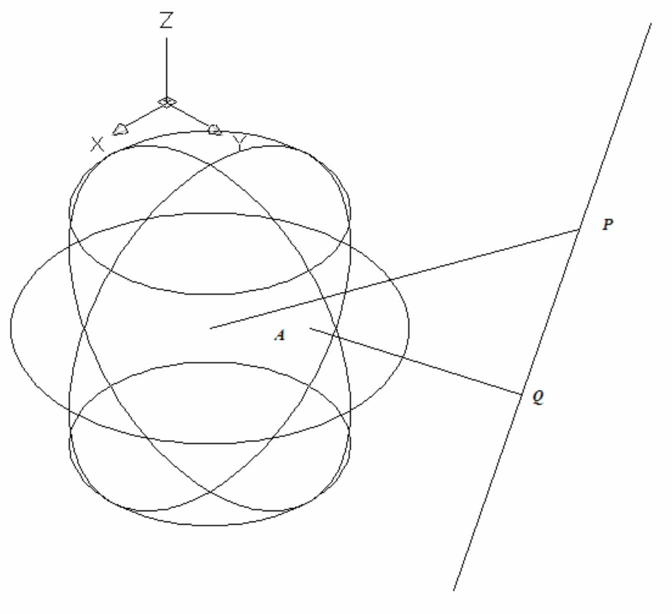

Fig. 11. Tolerance zone for 3D projection

Proof. Following the ideas in 2D, the tolerance zone is the intersection of three H-zones H_1, H_2, H_3. To find its boundaries, consider an arbitrary line $l(\theta, \varphi)$, whose spatial orientation is given in spherical polar coordinates by θ, φ (eee Figure 11). The intersection of H_i and $l(\theta, \varphi)$ is a segment of l. Using the same notation as in the 2D case, if Q is on this segment, the following inequality holds:

$$l \cos\theta \cos\varphi - r \leq \overrightarrow{PQ} \leq l \cos\theta \cos\varphi + r$$

Thus, as the oriented line l takes on all orientations in 3D space, the boundaries of tolerance zone are, following the argument used in 2D:

$$\rho = 2l \cos\theta \cos\varphi \pm 2r$$

□

3.4 Rotation

Finally, we consider rotation of a fat point point $P(x, y, z)$ relative to an origin at Q, about an arbitrary axis. The transformation can be described by an orthogonal matrix R:

$$P' - Q = (P - Q)R$$

where P' is the position of P after rotation.

When there is uncertainty in Q, denoted by ΔQ, $P' - Q - \Delta Q = (P - Q - \Delta Q)R$ holds for all possible positions of Q. We may rearrange this as

$$P' - Q = (P - Q)R + \Delta Q - \Delta QR.$$

Consider the term arising due to uncertainty, $\Delta Q - \Delta QR$. If the rotation angle is θ, the magnitude of this error term is $2\sin\theta/2$, and it makes an angle $\pi/2 - \theta/2$ relative to ΔQ. Thus, $\Delta Q - \Delta QR$ is obtained by rotation through an angle $\pi/2 - \theta/2$ and stretching by a ratio of $2\sin\theta/2$.

If we now consider the specific case where the uncertainty in Q is a sphere with radius r, the uncertainty after rotation is still a sphere, but with a radius $2r\sin\theta/2$.

Let us now further suppose that there is an uncertainty ΔP in the original point P. The total uncertainty is now $\Delta PR + \Delta Q - \Delta QR$. This can be viewed as the Minkowski sum of the uncertainty in P after rotation, with $\Delta Q - \Delta QR$. If ΔP is also represented by a sphere independently of ΔQ, the final result is a larger sphere of radius $r_p + 2r\sin\theta/2$, where r_p is the size of the spherical tolerance zone of P.

4 Conclusion and future work

We have provided definitions and constructions for various three dimensional geometric elements with tolerance, including points, lines, planes and spheres. We have then shown how to perform several geometric computations which take these tolerances into account, and provide suitable tolerance zones for the output. These calculations include the distance between two skew lines, and various reflections, projections, and rotations, with spherical tolerance zones. We have also discussed other computations with polyhedral tolerance zones.

Representation of tolerance zone boundaries is an important issue, and still needs further work. Boundaries of tolerance zones need to be restricted to certain particular shapes (e.g. spheres and polyhedra) if algorithms are to be efficiently implemented.

References

1. S. L. Abrams, W. Cho, C.-Y. Hu, T. Maekawa, N. M. Patrikalakis, E. C. Sherbrooke, and X. Ye. Efficient and reliable methods for rounded-interval arithmetic. *Computer-aided Design*, 30(8):657–665, 1998.
2. Chun-Yi Hu, Takashi Maekawa, Nicholas M. Patrikalakis, and Xiuzi Ye. Robust interval algorithm for surface intersections. *Computer-aided Design*, 29(9):617–627, 1997.
3. Chun-Yi Hu, Nicholas M. Patrikalakis, and Xiuzi Ye. Robust interval solid modelling part I: representations. *Computer-aided Design*, 28(10):807–817, 1996.
4. S.-M. Hu and J. Wallner. Error propagation through geometric transformations. *Journal for Geometry and Graphics*, 2(8):171–183, 2004.

5. Ku-Jin Kim. Minimum distance between a canal surface and a simple surface. *Computer-Aided Design*, 35(10):871–879, 2003.
6. H. Pottmann, B. Odehnal, M. Peternell, J. Wallner, and R. Ait Haddou. On optimal tolerancing in computer-aided design. In Ralph Martin and Wenping Wang, editors, *Proceedings of the Conference on Geometric Modeling and Processing (GMP-00)*, pages 347–363, Los Alamitos, April 10–12 2000. IEEE.
7. S. T. Tuohy, T. Maekawa, G. Shen, and N. M. Patrikalakis. Approximation of measured data with interval B-splines. *Computer-Aided Design*, 29(11):791–799, November 1997.
8. J. Wallner, H.-P. Schröcker, and S.-M. Hu. Tolerances in geometric constraint problems. *Reliable Computing*, 3(11):235–251, 2005.
9. Johannes Wallner, Rimvydas Krasauskas, and Helmut Pottmann. Error propagation in geometric constructions. *Computer-Aided Design*, 32(11):631–641, 2000.